

**SUSY and Higgs Signatures Implied by Cancellations in  $b \rightarrow s\gamma$** Ning Chen,<sup>1</sup> Daniel Feldman,<sup>2</sup> Zuowei Liu,<sup>1</sup> and Pran Nath<sup>3</sup>*<sup>1</sup>C.N. Yang Institute for Theoretical Physics,  
Stony Brook University, Stony Brook, NY 11794, USA**<sup>2</sup>Michigan Center for Theoretical Physics,  
University of Michigan, Ann Arbor, MI 48109, USA**<sup>3</sup>Department of Physics, Northeastern University, Boston, MA 02115, USA***Abstract**

Recent re-evaluations of the Standard Model (SM) contribution to  $\mathcal{B}r(b \rightarrow s\gamma)$  hint at a positive correction from new physics. Since a charged Higgs boson exchange always gives a positive contribution to this branching ratio, the constraint points to the possibility of a relatively light charged Higgs. It is found that under the HFAG constraints and with re-evaluated SM results large cancellations between the charged Higgs and the chargino contributions in supersymmetric models occur. Such cancellations then correlate the charged Higgs and the chargino masses often implying both are light. Inclusion of the more recent evaluation of  $g_\mu - 2$  is also considered. The combined constraints imply the existence of several light sparticles. Signatures arising from these light sparticles are investigated and the analysis indicates the possibility of their early discovery at the LHC in a significant part of the parameter space. We also show that for certain restricted regions of the parameter space, such as for very large  $\tan\beta$  under the  $1\sigma$  HFAG constraints, the signatures from Higgs production supersede those from sparticle production and may become the primary signatures for the discovery of supersymmetry.

**Introduction:** Recently a re-evaluation of the SM result for the branching ratio for the flavor changing neutral current (FCNC) process  $b \rightarrow s\gamma$  including NNLO corrections in QCD has been given [1]  $\mathcal{B}r(b \rightarrow s\gamma) = (3.15 \pm 0.23) \times 10^{-4}$ . This new estimate lies lower than the current experimental value which is given by the Heavy Flavor Averaging Group (HFAG) [2] along with the BABAR, Belle and CLEO experimental results:  $\mathcal{B}r(B \rightarrow X_s\gamma) = (352 \pm 23 \pm 9) \times 10^{-6}$ . The above result hints at a positive contribution to this process arising from new physics. It is known from the early days that the experimental value of the branching ratio  $b \rightarrow s\gamma$  is a very strong constraint on the parameter space of most classes of SUSY models [3, 4] (for more recent theoretical evaluations of  $\mathcal{B}r(b \rightarrow s\gamma)$  in supersymmetry see [5]). A positive contribution to  $\mathcal{B}r(b \rightarrow s\gamma)$  implies either the existence of a light charged Higgs exchange which always gives a positive contribution [6] or the existence of a light chargino which can give either a positive or a negative contribution [7]. A significant cancellation between the charged Higgs loop contribution and the chargino contribution implies that individual contributions from the charged Higgs loops and the gaugino loops must each be often multiples of their sum. Such cancellations then necessarily imply that some of the sparticles that enter in the supersymmetric contributions to the FCNC loops must be relatively light and thus should be accessible in early runs at the LHC.

In addition to the above, recently the difference between experiment and the standard model prediction of the anomalous magnetic moment of the muon,  $a_\mu = (g_\mu - 2)/2$  seem to converge [8] towards roughly a  $3\sigma$  deviation from the SM value. Thus the most recent analysis gives  $\delta a_\mu = a_\mu^{exp} - a_\mu^{SM}$  as [8]  $\delta a_\mu = (24.6 \pm 8.0) \times 10^{-10}$ . It is well known that supersymmetric electroweak contributions to  $g_\mu - 2$  can be as large or larger than the SM electroweak corrections [9]. Further, a large deviation of  $g_\mu - 2$  from the SM is a harbinger [10], for the observation of low lying sparticles [11–13] at colliders with the experimental data putting upper limits on some of the sparticle masses in SUGRA models [11]. The positive correction to  $b \rightarrow s\gamma$  which is of size  $(1 - 1.5)\sigma$  together with the  $3\sigma$  level deviation of  $g_\mu - 2$  from the standard model value points to the existence of some of the sparticles being light.

**Analysis:** In this work we investigate the implications of the revised constraints in the framework of supergravity grand unified models [14] following the analysis of [15] with the parameter space characterized by parameters  $m_0, m_{1/2}, A_0, \tan\beta, \text{sign}(\mu)$  where for Monte Carlo simulations we have assumed the following range:  $m_0 < 4 \text{ TeV}$ ,  $m_{1/2} < 2 \text{ TeV}$ ,

$|A_0/m_0| < 10$ , and  $1 < \tan\beta < 60$  with  $\mu > 0$  for three million candidate models. For the purpose of selecting viable models from the large scan, we impose the following set of constraints: (conservative bounds are given here to illustrate the constraining effects and also to account for experimental and theoretical uncertainties) (i) The 5-year WMAP data constrains the relic density of dark matter so that  $\Omega_{\text{DM}}h^2 = 0.1131 \pm 0.0034$  [16]. The bound  $0.0855 < \Omega_{\tilde{\chi}_1^0}h^2 < 0.1189$  [17] is taken; (ii) A  $3\sigma$  constraint for  $b \rightarrow s\gamma$  is taken around the HFAG value (a stricter constraint will be considered later); (iii) The 95% (90%) C.L. limit reported by CDF in  $\mathcal{B}r(B_s \rightarrow \mu^+\mu^-)$  is  $5.8 \times 10^{-8}$  ( $4.7 \times 10^{-8}$ ) [18] (we take  $\mathcal{B}r(B_s \rightarrow \mu^+\mu^-) < 10^{-6}$ ); (iv)  $\delta a_\mu \in (-5.7, 47) \times 10^{-10}$  is taken as in [19] (a stricter limit on  $\delta a_\mu$  will be discussed in the last section); (v) The following mass limits on light Higgs boson mass and on sparticle masses are imposed:  $m_h > 100$  GeV, (the current data sets limits for the MSSM case of  $m_h > 93$  GeV at 95% C.L. [21, 22])  $m_{\tilde{\chi}_1^\pm} > 104.5$  GeV,  $m_{\tilde{t}_1} > 101.5$  GeV,  $m_{\tilde{\tau}_1} > 98.8$  GeV, where  $h, \tilde{\chi}_1^\pm, \tilde{t}_1, \tilde{\tau}_1$  are the lightest Higgs boson, the chargino, the stop and the stau. For the calculations of the relic density of  $\tilde{\chi}_1^0$ , we use MicrOMEGAs [23] with sparticle and Higgs masses calculated by the RGE package SuSpect [24]. Evaluation of the branching ratio  $b \rightarrow s\gamma$  has been carried out with both MicrOMEGAs and SusyBSG [25]. The models that pass the above constraints are exhibited in Fig.(1).

**Cancellation of charged Higgs and chargino loop contributions to  $\mathcal{B}r(b \rightarrow s\gamma)$ :**

We discuss now in further detail the cancellation between the charged Higgs and the chargino loop contributions in the process  $b \rightarrow s\gamma$  and the implications of this cancellation, which may point to a light charged Higgs mass. The effective interaction that controls the  $b \rightarrow s\gamma$  decay is given by

$$H_{\text{eff}} = -2\sqrt{2}G_F V_{ts}^* V_{tb} \sum_{i=1}^8 C_i(Q) O_i(Q), \quad (1)$$

where  $V_{ts}, V_{tb}$  are the CKM matrix elements,  $O_i(Q)$  are the effective dimension six operators and  $C_i(Q)$  are the Wilson coefficients and  $Q$  is the renormalization group scale. The  $b \rightarrow s\gamma$  receives contributions only from  $C_2, C_7, C_8$  where the corresponding operators are  $O_2 = (\bar{c}_L \gamma^\mu b_L)(\bar{s}_L \gamma_\mu c_L)$ ,  $O_7 = (e/16\pi^2)m_b(\bar{s}_L \sigma^{\mu\nu} b_R)F_{\mu\nu}$ , and  $O_8 = (g_s/16\pi^2)m_b(\bar{s}_L \sigma^{\mu\nu} T^a b_R)G_{\mu\nu}^a$ . The dominant contribution arises from  $C_7$ , where to leading order  $C_7(m_b)$  is given by

$$C_7^{(0)}(m_b) = \eta^{16/23} C_7(M_W) + \frac{8}{3}(\eta^{16/23} - \eta^{14/23}) C_8(M_W) + C \quad (2)$$

and where  $\eta = \alpha_s(M_W)/\alpha_s(Q_b)$  and  $C (\simeq .175)$  arises from operator mixing. Now  $C_{7,8}$

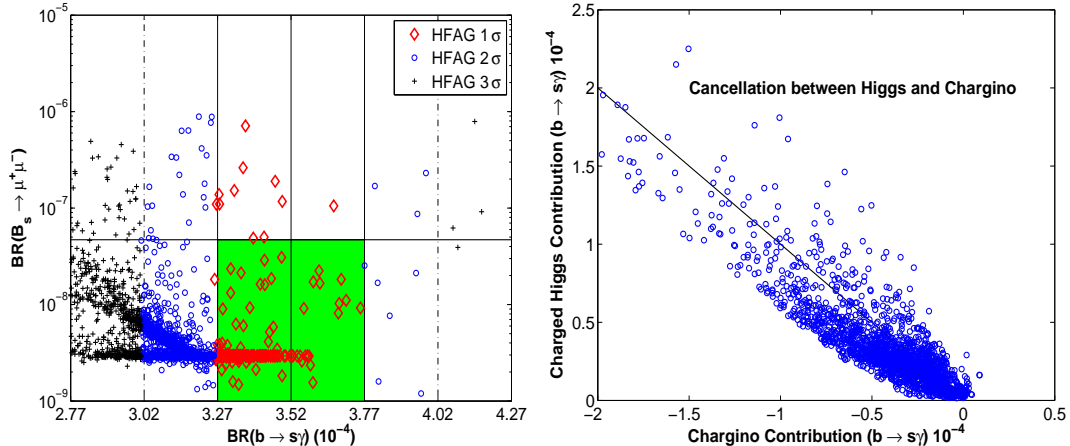


FIG. 1: Left: The shaded region are the models that survive the constraint  $\mathcal{B}r(B_s \rightarrow \mu^+\mu^-) < 4.7 \times 10^{-8}$  and the constraint  $\mathcal{B}r(b \rightarrow s\gamma) = 3.52 \pm 0.25$  as given by HFAG. Right: Charged Higgs contribution vs the chargino contribution. One finds that in most models the chargino exchange contributions are almost always negative and are strongly correlated with the charged Higgs contributions. The individual contributions from the charged Higgs and the chargino are computed using SusyBSG [25].

contain the standard model and new physics contributions so that

$$C_{7,8}(M_W) = C_{7,8}^W(M_W) + C_{7,8}^H(M_W) + C_{7,8}^X(M_W). \quad (3)$$

Here  $C_{7,8}^W$  is the standard model contribution arising from the W boson exchange,  $C_{7,8}^H$  is the supersymmetric contribution from the charged Higgs exchange and  $C_{7,8}^X$  is the contribution from the chargino exchange (see Fig(2)). In addition to the constraints on models arising from the  $\mathcal{B}r(b \rightarrow s\gamma)$  experiment, there are also constraints from the  $\mathcal{B}r(B_s \rightarrow \mu^+\mu^-)$  experiment. In the left panel of Fig.(1) we display the theoretical predictions in the  $\mathcal{B}r(B_s \rightarrow \mu^+\mu^-) - \mathcal{B}r(b \rightarrow s\gamma)$  plane, where the  $1\sigma$ ,  $2\sigma$ ,  $3\sigma$  corridors around the HFAG value of  $\mathcal{B}r(b \rightarrow s\gamma)$  are also exhibited. The analysis of the left panel Fig.(1) exhibits that the parameter space gets reduced in a significant way as the  $\mathcal{B}r(b \rightarrow s\gamma)$  constraint becomes more stringent. We now note that the sign of the chargino contribution  $C_{7,8}^X$  in Eq.(3) has a very dramatic effect on the size of the supersymmetric contribution. A positive contribution would add constructively with the charged Higgs contribution  $C_{7,8}^H$  while a negative contribution cancels partially the charged Higgs contribution reducing significantly the overall size. A numerical analysis shows that essentially for all the model points that lie in the  $3\sigma$  corridor around

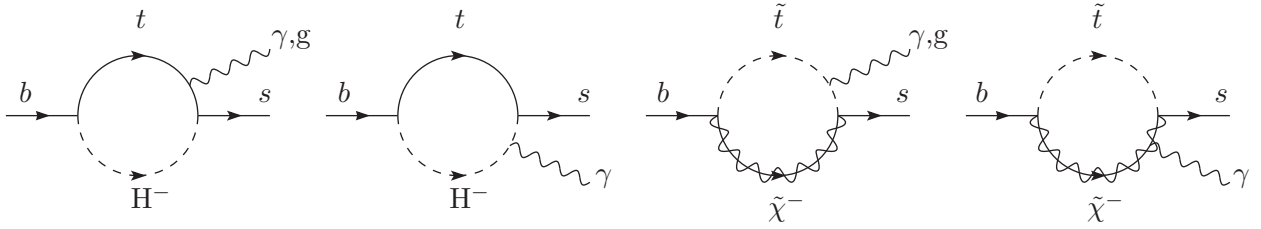


FIG. 2: Leading order contributions to  $b \rightarrow s\gamma$  from charged Higgs and chargino loops in supersymmetry.

the HFAG value the chargino contribution is negative and often large resulting in large cancellations. We exhibit this in the right panel of Fig.(1). One finds that a majority of the models are clustered around the standard model prediction of the  $b \rightarrow s\gamma$ . As discussed above this is a consequence of the *cancellation* between the charged Higgs and the chargino loop diagrams.

In the cancellations discussed above, the individual contributions from the charged Higgs loop and from the chargino loop are often much larger than the total SUSY contribution as exhibited in the right panel of Fig.(1). This implies that some of the sparticle spectrum must be light to allow for such large individual contributions in the branching ratio  $b \rightarrow s\gamma$ . The above also indicates that if the chargino is light, then correspondingly the charged Higgs must be correspondingly light to generate a large compensating contribution. So the cancellation phenomenon then strongly correlates the charged Higgs mass and the chargino mass in the region of large cancellations, i.e., in the region where the magnitude of the loop contributions from the chargino and from the charged Higgs are individually multiples of their sum.

An illustration of the correlation between the charged Higgs mass and  $\mathcal{B}r(b \rightarrow s\gamma)$  is given in the left panel of Fig.(3) in  $1\sigma$ ,  $2\sigma$ ,  $3\sigma$  corridors around the HFAG value. The analysis shows that a more stringent  $\mathcal{B}r(b \rightarrow s\gamma)$  constraint typically leads to a lighter charged Higgs mass. Further, as stated earlier the cancellation phenomenon also correlates the chargino mass to the charged Higgs mass. This is illustrated the right panel of Fig.(3). Specifically, here one finds that for the model points within HFAG  $1\sigma$ , a light charged Higgs mass often requires a light chargino mass to cancel the loop. So one expects to have light Higgs and a light

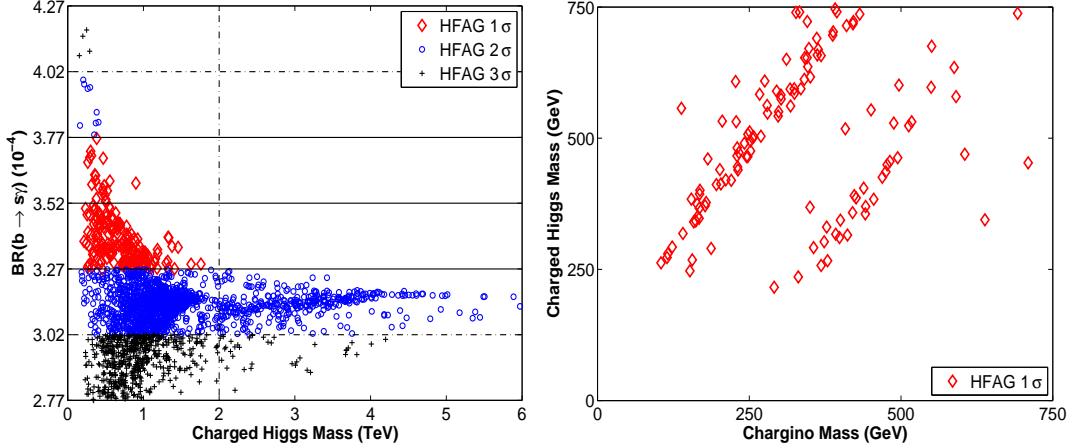


FIG. 3: Left: A display of the correlation between  $\mathcal{B}r(b \rightarrow s\gamma)$  and the charged Higgs boson mass showing the relative lightness of the charged Higgs boson mass in the  $1\sigma$ ,  $2\sigma$  and  $3\sigma$  corridors around the HFAG value. Right: A display of the model points in the charged Higgs mass vs the light chargino mass plane within the  $1\sigma$  corridor around the HFAG value in a large portion of the parameter space.

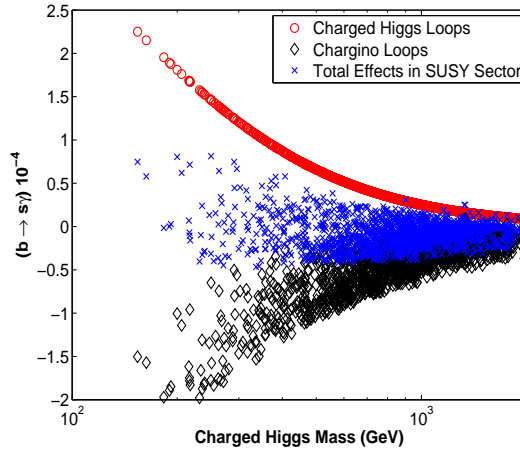


FIG. 4: A display of the contributions from the charged Higgs loop, the chargino loop (and also other gaugino loops), and the total effect beyond the SM.

chargino with comparable sizes. The cancellation between the charged Higgs contribution and the chargino contribution is also shown in Fig.(4) where the models with charged Higgs mass below 2 TeV are plotted. The charged Higgs contribution increases with decreasing charged Higgs mass, which forces the chargino contribution to increase in magnitude with decreasing charged Higgs mass in order that the total effect is consistent with the HFAG

constraints. We note that in the Two Higgs Doublet Model (THDM), the charged Higgs mass is also constrained from below, since there is no gaugino contributions to cancel the large positive contribution from the light charged Higgs. Thus, under the same constraints, the allowed charged Higgs mass can be much smaller in SUGRA models with a MSSM spectrum than in the THDM. We also note that the  $\mathcal{B}r(B_s \rightarrow \mu^+ \mu^-)$  constraint becomes important for the MSSM with large  $\tan \beta$ . The current experimental limit imposes a lower bound on the Higgs mass for models with large  $\tan \beta$ .

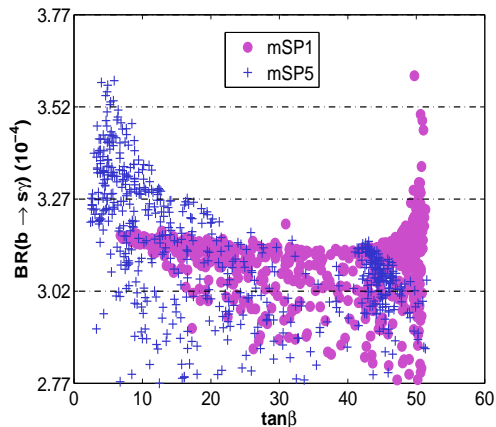


FIG. 5:  $b \rightarrow s\gamma$  vs  $\tan \beta$  for the mass patterns mSP1 and mSP5. The analysis of the figure shows that the  $1\sigma$   $b \rightarrow s\gamma$  constraint selects models in distinct regions of  $\tan \beta$ : (i) a region of low  $\tan \beta$  where the allowed models are mostly of type mSP5, and (ii) a region of large  $\tan \beta$  where the allowed the models are mostly of type mSP1.

A display of the  $\mathcal{B}r(b \rightarrow s\gamma)$  vs  $\tan \beta$  for mSP1 and mSP5 models<sup>1</sup> is given in Fig.(5) and the models that pass the  $1\sigma$  corridor cut on  $\mathcal{B}r(b \rightarrow s\gamma)$  around the experimental value are shown. One finds that in the region of the  $1\sigma$  HFAG corridor, the models from mSP1 where the lighter chargino is the NLSP have large  $\tan \beta$  values around 50, while the models from mSP5 where the lighter stau is the NLSP has much smaller  $\tan \beta$  values. We therefore collectively refer to models that reside in the  $\tan \beta$  region where  $\tan \beta < 40$  as low and high  $\tan \beta$  models, “LH  $\tan \beta$  models”. We segregate these LH models from those in which  $\tan \beta \geq 40$  denoting these as very high  $\tan \beta$  models, “VH  $\tan \beta$  models”, for all the models

<sup>1</sup> mSPs are supergravity mass hierarchies as defined in earlier works [15], where (mSP1,mSP5) have a (chargino, stau) NLSP respectively .

that fall within the  $1\sigma$  corridor around the HFAG value. We do so for all the different mass hierarchical patterns with mSP1 and mSP5 serving as illustrative examples. Typically the “LH  $\tan\beta$  models” are the ones in which the stau, the stop, or the gluino can be light, while the “VH  $\tan\beta$  models” are the ones where the chargino, or the Higgs is the next heavier particle than the LSP. Some implications of the updated constraints on Higgs masses are also given in [26–28].

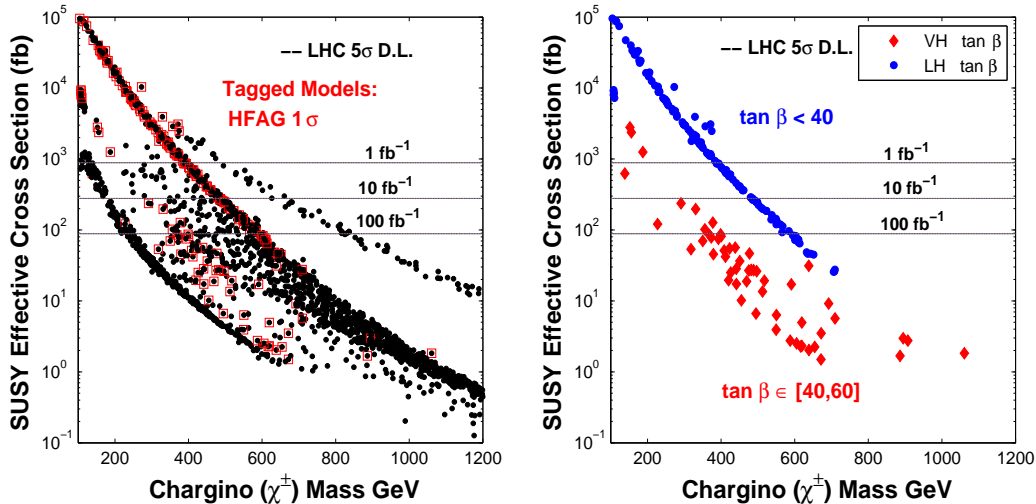


FIG. 6: Total SUSY signatures at  $\sqrt{s} = 14$  TeV analyzed with the SUSY detector cuts. Left: (circle,black) All models up to 1.2 TeV in the chargino masses, and (red,boxed) models within  $1\sigma$  corridor of the HFAG value. Right: Models separated out in  $\tan\beta$  that lie within  $1\sigma$  corridor of the HFAG. The dashed lines indicate the backgrounds,  $5\sqrt{\text{SM}}$ , for different luminosities.

**Production and Signatures of Sparticles:** In the following, we focus our analysis on the models that are favored by the  $b \rightarrow s\gamma$  constraint, namely, models that fall within a  $1\sigma$  corridor around the HFAG value. We discuss here the signatures of the  $2 \rightarrow 2$  SUSY processes. In the analysis we use SuSpect to create a SUSY Les Houches Accord (SLHA) [29] file which is then used as an input for PYTHIA [30] which computes the production cross sections and branching fractions, and for PGS [31] which simulates the LHC detector effects. The Level 1 (L1) trigger cuts based on the Compact Muon Solenoid detector specifications [32] are employed to analyze the LHC events. For our analysis of sparticles, we further impose the post trigger detector cuts as follows: We only select photons, electrons, and muons that have transverse momentum  $P_T > 10$  GeV and pseudorapidity  $|\eta| < 2.4$ , taus



jets that have  $P_T > 10$  GeV and  $|\eta| < 2.0$ , and other hadronic jets that have  $P_T > 60$  GeV and  $|\eta| < 3$ . We also require a large missing energy,  $\cancel{P}_T > 200$  GeV and at least two jets in an event to further suppress the Standard Model (SM) background. We will refer this set of cuts as ‘‘SUSY detector cuts’’ in the following analysis (for other recent works on signature analysis of SUGRA models see [33]).

We analyze the total number of events arising from the models in a  $1\sigma$  corridor around the HFAG results out of the  $3\sigma$  corridor using the SUSY detector cuts. The effective SUSY cross sections are then translated from the total number of events which are exhibited in Fig.(6). One finds that the models with low values of  $\tan\beta$  have strong SUSY signals since these models tend to have a light sparticle spectrum, e.g., a light stau, a light stop or even a light gluino. Most of the LH  $\tan\beta$  models discussed above can be probed at the LHC at  $100\text{ fb}^{-1}$  of integrated luminosity. It is found that the HFAG  $1\sigma$  constraint places a limit on the chargino mass of about 800 GeV for detectable models. We note that different models with different mass hierarchical spectra can have distinct SUSY signatures. For instance, models that have a light stau are rich in lepton signals, while models with a light stop tend to produce a high multiplicity of jet signals. Thus the search strategies for new physics at the LHC for such models are quite different, and a well designed search technique for every specific model will surely further improve the discovery reach. Nevertheless, the models that have low values of  $\tan\beta$  have strong SUSY production cross sections, and can be probed at the LHC. From the SUSY production analysis, one also finds that most of the VH  $\tan\beta$  models have much smaller SUSY cross sections.

**LHC Signatures in Higgs Production:** We discuss here the signatures of the Higgs bosons in MSSM (the CP-even Higgs  $H^0$ , the CP-odd Higgs  $A^0$ , and the charged Higgs  $H^\pm$ ) for the models that are within the  $1\sigma$  corridor of the HFAG value. Specially, we are interested in the parameter region where the  $\tan\beta$  value becomes very large. As discussed previously, the VH  $\tan\beta$  models within the  $1\sigma$  corridor of HFAG have less promising SUSY signals. However, the Higgs production can be much enhanced at very high  $\tan\beta$ . The dominant processes that lead to the production of the MSSM Higgs bosons at the LHC for  $\tan\beta \gg 1$  are the bottom quark annihilation process and the gluon fusion process [20] shown in Fig.(8) along with associated production processes with bottom quarks.

In our analysis, we focus on the hadronic  $\tau$  and jet production with bottom quark tagging, since the  $b\bar{b}$  and  $\tau^+\tau^-$  modes are the dominant decays of the MSSM Higgs bosons at large

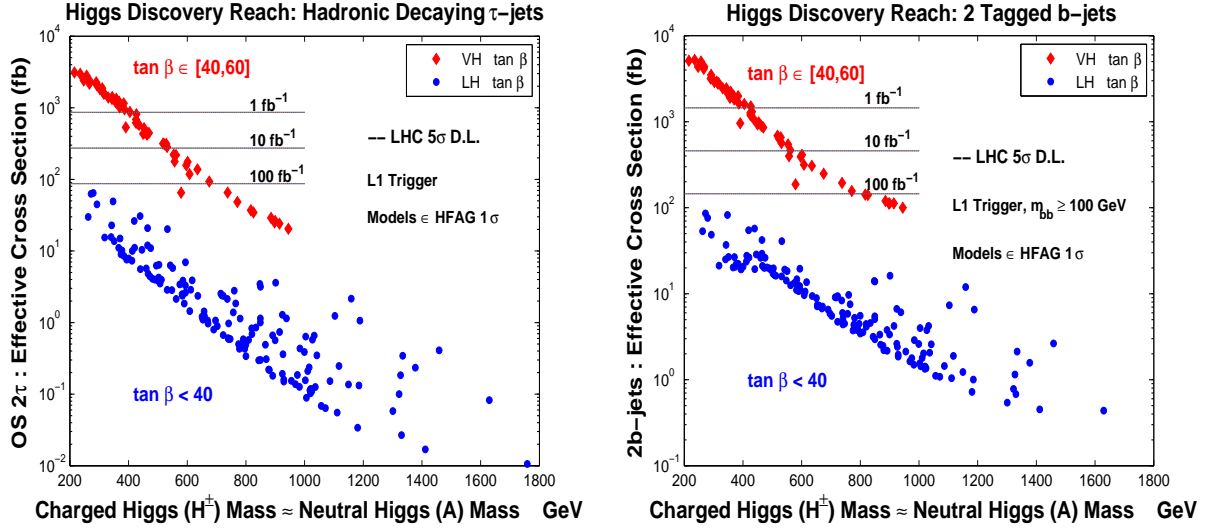


FIG. 7: Higgs signatures with b-tagged jets and hadronic  $\tau$ -jets at  $\sqrt{s} = 14$  TeV. The dashed lines indicate the backgrounds,  $5\sqrt{SM}$ , for different luminosities.

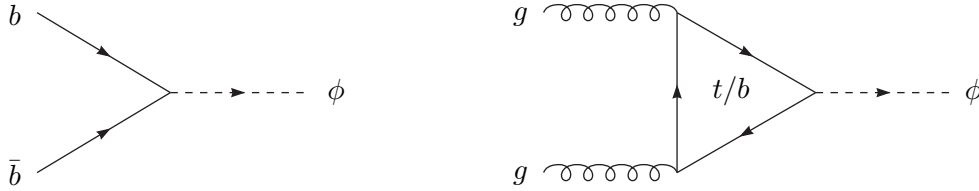


FIG. 8: Dominant leading order Higgs production diagrams via bottom quark annihilation and gluon fusion. For large  $\tan\beta$  the bottom quark annihilation can dominate the gluon fusion process in some regions of the parameter space.

$\tan\beta$ . We analyze the opposite sign (OS) di-tau signature and the 2b-jets signature using the L1 trigger cuts. For the 2b jet signatures, we also require the reconstructed invariant mass of these two b-tagged jets to be larger than 100 GeV. An analysis of the signatures for these models reveals the  $2\tau$  jet and the 2b jet channels to be two of the optimal channels for the discovery of the Higgs bosons as shown in Fig.(7). It is found that the HFAG  $1\sigma$  constraint places a limit on the charged Higgs mass about 1 TeV for the detectable models which can be probed with  $L = 100 \text{ fb}^{-1}$  or so at LHC. We note that for the region  $\tan\beta < 40$ , one needs much more luminosity to observe discoverable events from the Higgs production, and some of the models in this region may be even beyond the LHC reach in the Higgs production.

Thus the VH  $\tan\beta$  models are discoverable via Higgs production modes, while many of them have undetectable signals via sparticles productions. Thus the more optimal channels to discover supersymmetry in these VH  $\tan\beta$  models arise from Higgs production signals as they produce larger event rates than the event rates from SUSY production processes with R-parity odd particles. The associated production in which the Higgs bosons are produced along with one or two bottom quarks in the final states can be very useful for suppressing further the SM background [34–40]. One example of the associated production with one additional bottom quark in the final state is given in Fig.(11). For the hadronic  $\tau$  jets signature, we utilize both the 1-prong and the 3-prong hadronic  $\tau$ -jets [41] in our analysis. We note that the leptonic decay modes of the  $\tau$  lepton and a combined analysis of leptonic and hadronic decays may yield an even better discovery reach [42–44].

### Complementarity of Signatures from Sparticle Decays and from Higgs Decays:

Before discussing the issue of complementarity we discuss first the more stringent constraints arising from the recent revised analyses of  $g_\mu - 2$  which seem to converge [8] towards a  $3\sigma$  deviation from the standard model value. Fig.(9) illustrates a  $2\sigma$  corridor around the central values of  $\delta a_\mu$  and of the HFAG value of  $\mathcal{B}r(b \rightarrow s\gamma)$ . The analysis of Fig.(9) shows that the parameter space of allowed models is drastically reduced. A model point from the allowed set of models is discussed in further detail in the context of complementarity below.

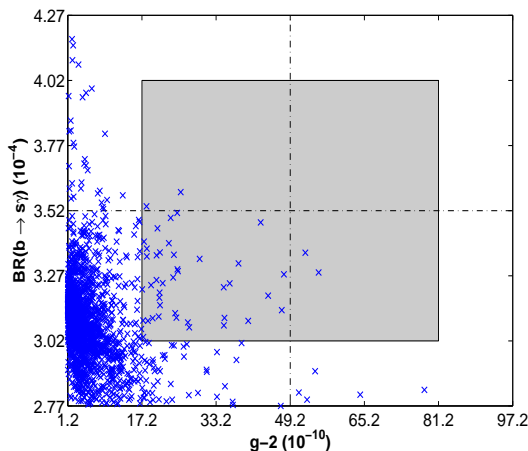


FIG. 9: Combined analysis with  $b \rightarrow s\gamma$  and  $g_\mu - 2$  constraints. Shaded regions are the  $2\sigma$  corridors from both constraints.

Next we point out a complementarity that exists between two main types of processes in the production and decays of new particles expected at the LHC. The first of the main types

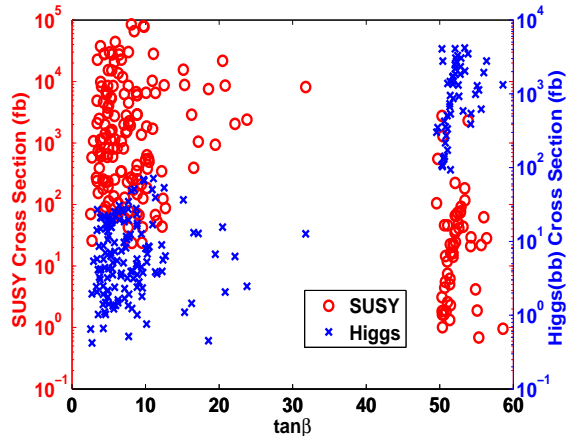


FIG. 10: A plot of both SUSY signatures and Higgs signatures for the models that fall within the  $1\sigma$  corridor around the HFAG value. The figure shows complementarity and inversion, in the sense that at low  $\tan\beta$  sparticle production cross sections dominate while at high  $\tan\beta$  the Higgs production cross sections dominate.

consists of those production processes which have in their final decay products an even number of massive LSPs (each an R-parity odd particle). These arise from the production and subsequent decay of an even number of R parity odd particles (due to R parity conservation) such as pairs of squarks or gauginos or both at the LHC. These processes are characterized by a large missing energy since the final states have at least two or more LSPs, which for the models considered are the lightest neutralinos. Thus here a larger missing transverse momentum is the smoking gun signature for the SUSY productions.

The second type of processes are those which do not contain pairs of LSPs and thus there is far less missing energy associated with these events. Such events are expected to arise from the production of the Higgs bosons where the dominant decay products are largely  $b\bar{b}$  and  $\tau^+\tau^-$ . The signals arising from the Higgs decays typically suffer from a large QCD background, since the  $\cancel{p}_T$  cut technique cannot be employed here which is efficient in suppressing the background for SUSY production. However, for models with very high  $\tan\beta$ , the Higgs production is enhanced and such model points can yield signals which can be discriminated from the QCD background. Thus we see that there is a complementarity between the signatures arising from the production and decay of the SUSY particles and from the Higgs particles, and this complementarity is exhibited in Fig.(10). Indeed for models with small  $\tan\beta$ , missing energy continues to be a dominant signal while for models

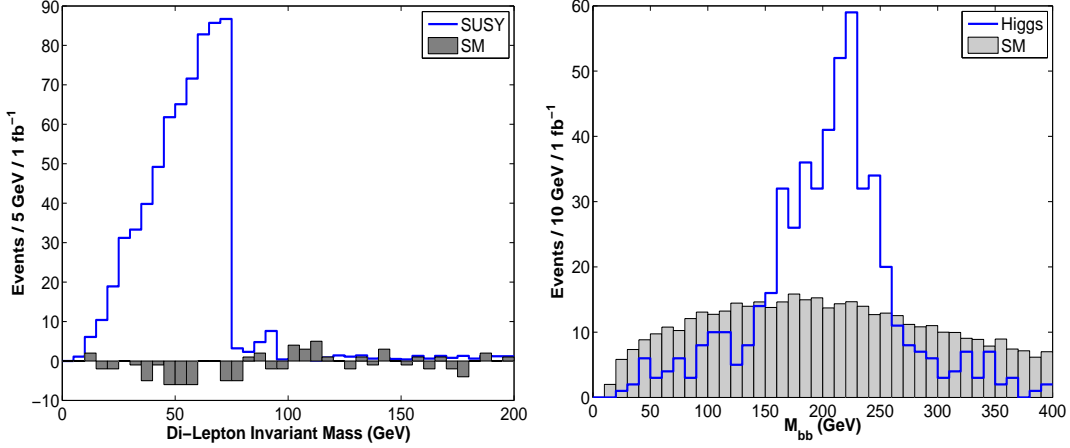


FIG. 11: Invariant mass distributions for SUSY and Higgs productions for two different models:  $(m_0, m_{1/2}, A_0, \tan\beta, \text{sign}(\mu)) = (70.4, 243.2, 685.6, 11, 1)$  (left panel);  $(1533.8, 216.4, 1750.3, 53.8, 1)$  (right panel) where all masses are in GeV. Left: The opposite sign di-lepton with flavor subtraction ( $e^+e^- + \mu^+\mu^- - e^+\mu^- - \mu^+e^-$ ), for the model that fall within  $1\sigma$  for both  $b \rightarrow s\gamma$  and  $g_\mu - 2$  constraints. In this model,  $M_{\tilde{\chi}_1^0} = 93$  GeV and  $M_{\tilde{\chi}_2^0} = 168$  GeV. The ending edge of the distribution indicates the mass difference ( $M_{\tilde{\chi}_2^0} - M_{\tilde{\chi}_1^0}$ ). Analysis is done with SUSY detector cuts. Shaded regions are the background  $N_{\text{SM}}$ . Right: Reconstruction of the two hardest b-tagged jets in 3 b-jets events of Higgs productions for the model that satisfies the HFAG  $1\sigma$ . The peak indicates the position of the Higgs boson mass. L1 trigger cuts are employed. Shaded regions are the background  $\sqrt{N_{\text{SM}}}$ .

with very high  $\tan\beta$  and within  $1\sigma$  corridor of HFAG value of  $b \rightarrow s\gamma$  the Higgs production and decay into  $b\bar{b}$  and  $\tau^+\tau^-$  can provide signatures which can supersede the signatures from sparticle production for the discovery of supersymmetry at the LHC.

A more detailed signal analysis on SUSY production and on Higgs production is given in Fig.(11). In the left panel of Fig.(11), the model considered is the one where stau is the NLSP and it shows a strong SUSY production signal which is rich in lepton final states. The lightest sparticles in this model besides the LSP are  $\tilde{\tau}$ ,  $\tilde{\ell}_R$ , so in the cascade decays of heavier gauginos, these sleptons can appear in the intermediate steps, for instance,  $\tilde{\chi}_2^0$  decays predominantly via  $\text{BR}(\tilde{\tau} + \tau) \sim 70\%$  and  $\text{BR}(\tilde{\ell}_R + \ell) \sim 20\%$ . The produced sleptons further decay into the LSP plus one lepton. Thus the reconstruction of the di-lepton events indicate the mass relations between the gauginos in the cascade decay chain due to the missing energy carried away by the LSP. In contrast, the invariant mass of the b-tagged jets

from the Higgs production gives rise to a resonance which points to the actual value of the Higgs boson mass as exhibited by the right panel of Fig.(11). As stated in the caption of Fig.(11) the cuts used in the left panel are the SUSY detector cuts which are discussed in the first paragraph of the section on "Production and signatures of sparticles". The right panel of Fig.(11) is analyzed with the standard L1 trigger cuts in PGS. The background in the left panel of Fig.(11) is suppressed by using flavor subtraction in reconstructing the dilepton events. For the right panel, the background is suppressed by reconstructing the two hardest b-tagged jets in the 3b events which can arise in the associated production modes of Higgs bosons. The associated production where the Higgs bosons are produced along with additional b-tagged jets is instrumental in suppressing the background.

**Conclusion:**  $\mathcal{B}r(b \rightarrow s\gamma)$  in the standard model re-evaluated by the inclusion of NNLO corrections falls below the central HFAG value by about  $(1 - 1.5)\sigma$  hinting at a positive contribution from the supersymmetric sector. The obvious candidate for a positive contribution is the charged Higgs exchange. On the other hand the chargino exchange contributions can produce either a positive or a negative contribution. Further, the recent re-evaluations of the  $g_\mu - 2$  indicate about a  $3.1\sigma$  deviations from the standard model pointing to the possibility of a light chargino. A detailed investigation of the parameter space of supergravity models reveals that most model points that satisfy both the  $\mathcal{B}r(b \rightarrow s\gamma)$  and the  $g_\mu - 2$  constraints produce both a light charged Higgs and a light chargino with a cancellation between the charged Higgs loops and the chargino loops indicating the existence of some of the sparticle masses, specifically the chargino, charged Higgs and the stop being light. We have emphasized the importance of studying simultaneously sparticle and Higgs production. The implications of these results for early SUSY discovery at the LHC were discussed and it is shown that some of the sparticles can be discovered in runs with low luminosity.

*Acknowledgments:* This research is supported in part by NSF grant PHY-0653342 (Stony Brook), DOE grant DE-FG02-95ER40899 (MCTP), and NSF grant PHY-0757959 (North-eastern University). NC and ZL would like to thank Alex Mitov and Robert Shrock for helpful discussions.

- 
- [1] M. Misiak *et al.*, Phys. Rev. Lett. **98** (2007) 022002.
- [2] E. Barberio *et al.* [Heavy Flavor Averaging Group], arXiv:0808.1297 [hep-ex].
- [3] S. Bertolini, F. Borzumati, A. Masiero and G. Ridolfi, Nucl. Phys. B **353**, 591 (1991).
- [4] P. Nath and R. L. Arnowitt, Phys. Lett. B **336**, 395 (1994); F. Borzumati, M. Drees and M. M. Nojiri, Phys. Rev. D **51**, 341 (1995).
- [5] G. Degrossi, P. Gambino and G. F. Giudice, JHEP **0012** (2000) 009; F. Borzumati, C. Greub, T. Hurth and D. Wyler, Phys. Rev. D **62**, 075005 (2000) D. A. Demir and K. A. Olive, Phys. Rev. D **65**, 034007 (2002); A. J. Buras *et al.*, Nucl. Phys. B **659** (2003) 3; M. E. Gomez, T. Ibrahim, P. Nath and S. Skadhauge, Phys. Rev. D **74** (2006) 015015; G. Degrossi, P. Gambino and P. Slavich, Phys. Lett. B **635** (2006) 335.
- [6] J. L. Hewett, Phys. Rev. Lett. **70**, 1045 (1993); V. D. Barger, M. S. Berger and R. J. N. Phillips, Phys. Rev. Lett. **70**, 1368 (1993).
- [7] R. Garisto and J. N. Ng, Phys. Lett. B **315**, 372 (1993).
- [8] M. Davier, A. Hoecker, B. Malaescu, C. Z. Yuan and Z. Zhang, arXiv:0908.4300 [hep-ph].
- [9] T. C. Yuan, R. L. Arnowitt, A. H. Chamseddine and P. Nath, Z. Phys. C **26**, 407 (1984); D. A. Kosower, L. M. Krauss and N. Sakai, Phys. Lett. B **133**, 305 (1983); J. L. Lopez, D. V. Nanopoulos and X. Wang, Phys. Rev. D **49**, 366 (1994); J. L. Lopez, D. V. Nanopoulos and X. Wang, Phys. Rev. D **49**, 366 (1994). T. Moroi, Phys. Rev. D **53**, 6565 (1996).
- [10] A. Czarnecki and W. J. Marciano, Phys. Rev. D **64**, 013014 (2001).
- [11] U. Chattopadhyay and P. Nath, Phys. Rev. Lett. **86**, 5854 (2001).
- [12] L. L. Everett, G. L. Kane, S. Rigolin and L. T. Wang, Phys. Rev. Lett. **86**, 3484 (2001).
- [13] J. L. Feng and K. T. Matchev, Phys. Rev. Lett. **86**, 3480 (2001); E. A. Baltz and P. Gondolo, Phys. Rev. Lett. **86**, 5004 (2001); T. Ibrahim, U. Chattopadhyay and P. Nath, Phys. Rev. **D64**, 016010(2001); J. Ellis, D.V. Nanopoulos, K. A. Olive, Phys. Lett. B **508**, 65 (2001); R. Arnowitt, B. Dutta, B. Hu, Y. Santoso, Phys. Lett. B **505**, 177 (2001); S. P. Martin, J. D. Wells, Phys. Rev. D **64**, 035003 (2001); H. Baer, C. Balazs, J. Ferrandis, X. Tata, Phys.Rev.**D64**: 035004, (2001).
- [14] A. H. Chamseddine, R. Arnowitt and P. Nath, Phys. Rev. Lett. **49**, 970 (1982); P. Nath, R. Arnowitt and A. H. Chamseddine, Nucl. Phys. B **227**, 121 (1983); L. J. Hall, J. D. Lykken

- and S. Weinberg, Phys. Rev. D **27** (1983) 2359.
- [15] D. Feldman, Z. Liu and P. Nath, Phys. Rev. Lett. **99**, 251802 (2007); D. Feldman, Z. Liu and P. Nath, JHEP **0804**, 054 (2008).
- [16] E. Komatsu *et al.* [WMAP Collaboration], Astrophys. J. Suppl. **180**, 330 (2009).
- [17] D. N. Spergel *et al.*, astro-ph/0603449.
- [18] T. Aaltonen *et al.* [CDF Collaboration], Phys. Rev. Lett. **100**, 101802 (2008).
- [19] A. Djouadi, M. Drees and J. L. Kneur, JHEP **0603**, 033 (2006).
- [20] A. Djouadi, M. Spira and P. M. Zerwas, Phys. Lett. B **264**, 440 (1991); M. Spira, A. Djouadi, D. Graudenz and P. M. Zerwas, Nucl. Phys. B **453** (1995) 17.
- [21] S. Dawson, C. B. Jackson, L. Reina and D. Wackerroth, Mod. Phys. Lett. A **21**, 89 (2006).
- [22] The LEP Higgs Working Group, LHWG-Note 2004-01 (August 2004).
- [23] G. Belanger, F. Boudjema, A. Pukhov and A. Semenov, Comput. Phys. Commun. **176**, 367 (2007).
- [24] A. Djouadi, J. L. Kneur and G. Moultaka, Comput. Phys. Commun. **176**, 426 (2007).
- [25] G. Degrandi, P. Gambino and P. Slavich, Comput. Phys. Commun. **179**, 759 (2008).
- [26] D. Feldman, Z. Liu and P. Nath, Phys. Lett. B **662**, 190 (2008).
- [27] G. Barenboim, P. Paradisi, O. Vives, E. Lunghi and W. Porod, JHEP **0804**, 079 (2008).
- [28] B. Dudley and C. Kolda, arXiv:0901.3337 [hep-ph].
- [29] P. Skands *et al.*, JHEP **0407**, 036 (2004).
- [30] T. Sjostrand, S. Mrenna, P. Skands, JHEP **0605**, 026 (2006).
- [31] <http://www.physics.ucdavis.edu/~conway/research/software/pgs/pgs4-general.htm>
- [32] CMS Collaboration, CERN/LHCC 2006-001 (2006).
- [33] R. Arnowitt *et al.*, Phys. Lett. B **649**, 73 (2007); U. Chattopadhyay, D. Das, A. Datta and S. Poddar, Phys. Rev. D **76**, 055008 (2007); H. Baer, A. Mustafayev, E. K. Park and X. Tata, JHEP **0805**, 058 (2008); D. Feldman, Z. Liu and P. Nath, Phys. Rev. D **78**, 083523 (2008); Phys. Rev. D **80**, 015007 (2009); B. Altunkaynak, P. Grajek, M. Holmes, G. Kane and B. D. Nelson, JHEP **0904**, 114 (2009); D. Feldman, Z. Liu, P. Nath and B. D. Nelson, Phys. Rev. D **80**, 075001 (2009); S. Bhattacharya, U. Chattopadhyay, D. Choudhury, D. Das and B. Mukhopadhyaya, arXiv:0907.3428 [hep-ph]; H. Baer, V. Barger, A. Lessa and X. Tata, arXiv:0907.1922 [hep-ph]; D. Feldman, arXiv:0908.3727 [hep-ph].
- [34] C. Balazs, J. L. Diaz-Cruz, H. J. He, T. M. P. Tait and C. P. Yuan, Phys. Rev. D **59**, 055016



- (1999).
- [35] D. J. Miller, S. Moretti, D. P. Roy and W. J. Stirling, Phys. Rev. D **61**, 055011 (2000).
  - [36] J. M. Campbell, R. K. Ellis, F. Maltoni and S. Willenbrock, Phys. Rev. D **67**, 095002 (2003).
  - [37] F. Maltoni, Z. Sullivan and S. Willenbrock, Phys. Rev. D **67**, 093005 (2003).
  - [38] R. V. Harlander and W. B. Kilgore, Phys. Rev. D **68**, 013001 (2003).
  - [39] A. Belyaev, A. Blum, R. S. Chivukula and E. H. Simmons, Phys. Rev. D **72**, 055022 (2005);  
U. Aglietti *et al.*, arXiv:hep-ph/0612172.
  - [40] M. S. Carena, S. Heinemeyer, C. E. M. Wagner and G. Weiglein, Eur. Phys. J. C **45**, 797 (2006).
  - [41] M. Guchait, R. Kinnunen and D. P. Roy, Eur. Phys. J. C **52**, 665 (2007).
  - [42] S. Dawson, D. Dicus, C. Kao and R. Malhotra, Phys. Rev. Lett. **92**, 241801 (2004).
  - [43] C. Kao, D. A. Dicus, R. Malhotra and Y. Wang, Phys. Rev. D **77**, 095002 (2008).
  - [44] C. Lampen, ATL-PHYS-PROC-2009-122 (ATLAS Notes).